Qin et al. *Zool. Res.* 2025, 46(4): 750−760
https://doi.org/10.24272/j.issn.2095-8137.2025.033
https://cstr.cn/32248.14.zr.2025.033

ZR | Zoological Research

Article Open Access

RNF122 targets STING for ubiquitination at residues K95, K117, and K155 to regulate antiviral responses in a teleost fish

Xiao-Wei Qin[1], Chuan-Rui Li[1], Min-Cong Liang[1], Tian-Hao Li[1], Yan-Lin You[1], Shao-Ping Weng[1], Chang-Jun Guo[1,*], Jian-Guo He[1]

[1] *School of Life Sciences*, *State Key Laboratory for Biocontrol/Southern Marine Science and Engineering Guangdong Laboratory (Zhuhai)*, *Guangdong Province Key Laboratory for Aquatic Economic Animals* & *Guangdong Provincial Observation and Research Station for Marine Ranching of the Lingdingyang Bay*, *Sun Yat-sen University*, *Guangzhou*, *Guangdong* 510275, *China*

ABSTRACT

Ring finger protein 122 (RNF122), an E3 ubiquitin ligase, orchestrates antiviral immune responses in mammals by targeting retinoic acid-inducible gene 1 and melanoma differentiation-associated gene 5 for ubiquitination. However, its functional relevance in teleosts has yet to be clearly defined, particularly regarding the identification of substrate-specific regulatory sites. This study characterized RNF122 from mandarin fish (*Siniperca chuatsi*), termed *sc*RNF122, and investigated its regulatory impact on stimulator of interferon genes (STING)-mediated antiviral signaling. Results showed that *sc*RNF122 expression was up-regulated in response to mandarin fish ranavirus (MRV) infection, and its overexpression suppressed *sc*STING-mediated interferon (IFN) production and enhanced MRV replication. Co-immunoprecipitation confirmed a direct interaction between *sc*RNF122 and *sc*STING. Functional assays demonstrated that *sc*RNF122 facilitated *sc*STING degradation through the ubiquitin-proteasome pathway, a process impeded by MG132 treatment. Ubiquitination analyses of various *sc*STING mutants revealed that *sc*RNF122 catalyzed *sc*STING ubiquitination at K95, K117, and K155 residues. Moreover, *sc*RNF122 significantly impaired *sc*STING-dependent antiviral responses by engaging negative regulatory elements within the signaling cascade. Overall, *sc*RNF122 was identified as a negative modulator of STING-mediated IFN signaling in mandarin fish, diminishing STING-dependent antiviral activity and promoting its degradation via the ubiquitin-proteasome pathway at lysine residues K95, K117, and K155. These findings provide mechanistic insight into the post-translational control of STING in teleosts and establish a foundation for future investigations into antiviral immune regulation.

Keywords: RNF122; STING; Ubiquitination; Interferon; Innate immunity

INTRODUCTION

The innate immune system constitutes the first line of defense against viral pathogens, with the stimulator of interferon genes (STING) pathway serving as a primary sensor of viral DNA. STING, a transmembrane adapter protein, plays an essential role in detecting pathogenic cytoplasmic DNA (Ishikawa & Barber, 2008; Zhong et al., 2008) and initiating downstream signaling cascades that culminate in the production of type I interferon (IFN-I) and proinflammatory cytokines, thereby triggering a robust antiviral immune response (Ishikawa et al., 2009; Phelan et al., 2020). This DNA-sensing axis is a crucial component of host recognition and response to viral infections, and its activity is tightly regulated through various post-translational modifications, including phosphorylation and ubiquitination (Hopfner & Hornung, 2020). Among these modifications, ubiquitination has emerged as a critical modulator of STING function, exerting context-dependent effects that either enhance or suppress signaling output (Bhoj & Chen, 2009; Pan et al., 2023).

Recent studies have highlighted RNF122, an E3 ubiquitin ligase, as a pivotal negative regulator of antiviral responses in mammals. RNF122 mediates proteasomal degradation of retinoic acid-inducible gene 1 (RIG-I) by targeting its CARD, thereby dampening RIG-I-dependent signaling (Wang et al., 2016). Additionally, during porcine reproductive and respiratory syndrome viral infection, non-canonical viral proteins such as Nsp1a, Nsp7, and Nsp9 induce RNF122

Received: 20 March 2025; Accepted: 26 May 2025; Online: 27 May 2025
Foundation items: This work was supported by the National Key Research and Development Program of China (2022YFE0203900, 2024YFD2401101), China Agriculture Research System (CARS-46), National Natural Science Foundation of China (32473201), and Guangdong S&T Program (2022B1111030001, 2024B1212040007)
*Corresponding author, E-mail: gchangj@mail.sysu.edu.cn

expression, leading to the ubiquitination and degradation of melanoma differentiation-associated gene 5 (MDA-5), thereby facilitating viral replication (Sun et al., 2022). Despite these insights, the role of RNF122 in teleost fish remains incompletely characterized, particularly in relation to substrate recognition and site-specific regulatory activity (Sun et al., 2022).

The mandarin fish (*Siniperca chuatsi*) is an economically important species in Chinese aquaculture (Yu et al., 2023), yet its intensive cultivation has led to increased susceptibility to infectious outbreaks. Among these, mandarin fish ranavirus (MRV), a double-stranded DNA virus belonging to the *Ranavirus* genus of the *Iridoviridae* family, presents a major threat to aquaculture sustainability (Dong et al., 2017). Elucidating the mechanisms by which innate immunity regulates viral control in this species is crucial for advancing fish health management and antiviral intervention strategies. This study investigated the immunoregulatory function of *S. chuatsi* RNF122 (*sc*RNF122) in modulating STING-mediated antiviral immune responses and identified the specific lysine residues on STING targeted for ubiquitination. The results of this study offer valuable insights into the regulatory mechanisms underlying STING-mediated signaling in teleost fish.

MATERIALS AND METHODS

Animals, cells, and viruses

Mandarin fish (average weight 50 g) were obtained from a farm located in Guangdong Province, China. Before experimentation, the fish were acclimatized for two weeks in a recirculating freshwater system maintained at 27°C. All animal procedures were performed in accordance with the regulations for animal experimentation in Guangdong Province, China, and permitted by the Ethics Committee of Sun Yat-sen University (approval no. 2023121901). Mandarin fish fry (MFF-1) cells were cultured in Dulbecco's Modified Eagle Medium (DMEM; Gibco, USA) supplemented with 10% fetal bovine serum (FBS; Gibco, USA) at 27°C in a humidified atmosphere containing 5% CO_2 (Dong et al., 2008). Fathead minnow (FHM) cells (ATCC CCL-42) were maintained in M199 medium supplemented with 10% FBS at 27°C (Li et al., 2024). Human normal liver cells (L02) were maintained in DMEM supplemented with 10% FBS at 37°C. The MRV strain NH-1609 (MG941005) was isolated from mandarin fish in Nanhai, Guangdong, China, and stored in our laboratory (Li et al., 2024).

Reagents and antibodies

Proteasome inhibitor MG132, cycloheximide (CHX), 3-methyladenine (3-MA), and chloroquine (CQ) were purchased from MedChemExpress (USA). Iodoacetamide (IAA) was obtained from Cell Signaling Technology (CST, USA). Mouse monoclonal antibodies against C-Myc and Flag were sourced from Sigma-Aldrich (1:5 000, USA). Anti-HA monoclonal antibody was obtained from CST (1:1 000, USA) and anti-GAPDH antibody was procured from Abways (1:3 000, China). Rabbit polyclonal anti-mrvORF097L antibody (1:5 000) was generated in our laboratory (Pan et al., 2024). Horseradish peroxidase (HRP)-conjugated goat anti-mouse IgG (H+L) and goat anti-rabbit IgG (H+L) secondary antibodies were obtained from Promega (1:5 000, USA).

Bioinformatic analyses

Protein domains of *sc*RNF122 were predicted using the SMART database (http://smart.embl-heidelberg.de/) in Genomic Mode (Letunic et al., 2021). Protein sequences were retrieved from GenBank (Benson et al., 2013) and RefSeq (O'Leary et al., 2016) for phylogenetic analysis. Sequences were aligned using ClustalW in MEGA v.11.0.13 (Tamura et al., 2021). The phylogenetic tree was constructed using the neighbor-joining method with 1 000 bootstrap replications under the Jones-Taylor-Thornton (JTT) model and complete deletion settings. Tree visualization was performed using iTOL (https://itol.embl.de/) (Letunic & Bork, 2024). Illustrative elements were prepared using the Generic Diagramming Platform (Jiang et al., 2025). Protein amino acid sequences retrieved from GenBank and RefSeq were aligned using Dynamic Alignment with default parameters in DNAMAN v.9.0.

Plasmid construction and cell transfection

Total RNA was extracted using an SV Total RNA Isolation Kit (Promega, USA) and reverse transcribed into first-strand cDNA using an Evo M-MLV qPCR RT Kit (Accurate Biology, China), as described in previous research (Qin et al., 2020). The *sc*RNF122 and *sc*STING gene fragments were cloned and inserted into pCMV-Myc-N and pCMV-Flag-N vectors (Takara, Japan), respectively. Various *sc*STING gene segments, including *sc*STING(1–94), *sc*STING(1–121), *sc*STING(1–116), *sc*STING(1–135), *sc*STING(1–140), *sc*STING(1–180), *sc*STING(181–417), *sc*STINGCKR(1–161) 155K, *sc*STINGCKR(1–141)135K, *sc*STINGCKR(1–128)122K, *sc*STINGCKR(1–123)117K, and *sc*STINGCKR(1–101)95K, were processed. In addition, multiple *sc*STING constructs, including Flag-*sc*STING mutants (e.g., *sc*STING(1–180)KR, *sc*STINGCKR, *sc*STINGCKRK20, *sc*STINGK20R, *sc*STINGCKRK95, *sc*STINGK95R *sc*STINGCKRK117, *sc*STINGK117R, *sc*STINGCKRK122, *sc*STINGCKRK135, *sc*STINGCKRK155, *sc*STINGK155R, and *sc*STINGK95/117/155R), were produced by Beijing Tsingke Biotechnology (China). The primers used for gene cloning, which incorporated restriction enzyme sites, are detailed in Supplementary Table S1. Transfection of the plasmids into FHM cells was carried out using Fugene HD (Promega, USA), while MFF-1 cells were transfected using Transfect EZ 3000 Plus (eLGbio, China), following the manufacturer's protocols.

Reverse transcription-quantitative real-time polymerase chain reaction (RT-qPCR)

RT-qPCR was performed using SYBR Premix ExTaq (Takara, Japan) on a LightCycler 480 system (Roche Diagnostics, Switzerland), following previously established protocols (Qin et al., 2020). Expression levels of immune-related and viral genes were normalized to *scβ-actin*. Primer sequences for *scRNF122*, *scSTING*, *scβ-actin*, *mrvMCP*, *mrvICP18*, and mrvDNA polymerase (*mrvDNA-Poly*) genes are provided in Supplementary Table S2.

Tissue expression profiling and dual-luciferase reporter assays

To determine the tissue-specific distribution of *sc*RNF122 in healthy fish, total RNA was extracted from blood, brain, gills, fins, spleen, intestine, head kidney, middle kidney, hind kidney, fat, heart, liver, and muscle, as previously described (Qin et al., 2020). RT-qPCR was employed to assess transcript levels across tissues using the primer sets listed in Supplementary Table S2. For promoter activity analysis, luciferase assays were performed using the Dual-Luciferase Reporter Assay System (Promega, USA), following

established procedures (Qin et al., 2020). All experiments were conducted in triplicate, with data representing the mean of at least three independent experiments.

Co-immunoprecipitation (Co-IP) and western blot (WB) analysis

The Co-IP and WB procedures were carried out as previously reported (Qin et al., 2020). Protein bands were visualized using High-sig ECL western blotting substrate (Tanon, China) and imaged with the Amersham ImageQuant 800 system (Cytiva, USA).

Viral titer determination

Virus titers in MFF-1 cells were quantified according to previously described protocols (Zeng et al., 2021). In brief, cells were seeded into 96-well plates and incubated until reaching a confluence of over 80%. Serial 10-fold dilutions of MRV-containing samples were prepared and inoculated into eight replicate wells per dilution. Negative control wells were inoculated with 100 μL of virus-free culture medium. Plates were incubated at 27°C for seven days, after which the number of positive and negative wells was recorded. $TCID_{50}$ values were calculated using the Spearman-Karber method (Reed & Muench, 1938).

Statistical analysis

Statistical analyses were performed using SPSS v.20. One-way analysis of variance (ANOVA) was applied to assess differences between groups. Data are presented as mean ± standard deviation (SD), derived from three independent experiments performed in triplicate. Statistical significance was defined as *: $P<0.05$ and **: $P<0.01$ compared to the controls.

RESULTS

Characterization of *sc*RNF122 and its promotion of MRV replication

Sequence alignment of mandarin fish transcriptomic data revealed a transcript (XM_044191507.1) with high homology to RNF122. The corresponding gene was cloned, resulting in the acquisition of a 468 bp full-length cDNA, designated *sc*RNF122. SMART domain analysis and amino acid sequence examination indicated that *sc*RNF122 encodes a 17.6 kDa protein containing a transmembrane region (TM) and canonical RING-finger domain (RING) (Figure 1A). Phylogenetic analysis positioned *sc*RNF122 within the same clade as RNF122 proteins from other fish species, distinct from other RNF122 family members (Figure 1B; Supplementary Table S3). Expression profiling of *sc*RNF122 across multiple tissues in healthy mandarin fish showed that *sc*RNF122 was broadly expressed, with the highest expression observed in spleen —a crucial immune tissue in fish —approximately 27-fold higher than that in muscle (Figure 1C), suggesting potential involvement in immune response.

To investigate whether *sc*RNF122 participates in the host response to viral infection, its transcriptional dynamics were monitored in MFF-1 cells following MRV challenge. Results showed that *sc*RNF122 expression increased in a time-dependent manner, exhibiting 47-, 141-, and 158-fold up-regulation at 24, 36, and 48 h post-infection, respectively (Figure 1D), indicating potential involvement in viral pathogenesis. Functional analysis was performed by overexpressing *sc*RNF122 in MFF-1 cells, followed by MRV infection. Cells transfected with either *sc*RNF122 or the control vector (pCMV-Myc) and subsequently infected with MRV were collected for RT-qPCR, WB, and $TCID_{50}$ assays. Overexpression of *sc*RNF122 (Figure 1E) led to a marked decrease in *scIFN-h* expression (Figure 1F), whereas transcription of MRV genes *mrvMCP*, *mrvICP18*, and *mrvDNA-Poly* was significantly elevated compared to controls (Figure 1G–I). Correspondingly, viral titers (Figure 1J) and levels of the viral protein mrvORF097L (Figure 1K, L) were markedly increased in the *sc*RNF122 group compared to controls. These observations indicate that *sc*RNF122 inhibits the production of IFN and enhances MRV replication.

***sc*RNF122 targets the 141–417 amino acid region of STING to suppress IFN signaling**

To explore the regulatory role of *sc*RNF122 in STING-mediated IFN signaling, dual-luciferase reporter assays were conducted following co-transfection of cells with plasmids encoding *sc*RNF122 and *sc*STING. Results showed that when both proteins were co-expressed, *sc*RNF122 exerted a dose-dependent inhibitory effect on *sc*STING-induced IFN-β-luciferase activity (Figure 2A, B). Furthermore, expression levels of IFN-I-related genes (*scIFN-h*, *scMx*, and *scISG15*; Figure 2C–E) and the pro-inflammatory cytokine *scTNF-α* (Figure 2F) were significantly decreased in cells co-expressing *sc*STING and *sc*RNF122 compared to those co-expressing *sc*STING and the pCMV-Myc control vector ($P<0.01$). These findings suggest that *sc*RNF122 acts as a negative regulator of *sc*STING-mediated IFN signaling.

To determine the region of scSTING targeted by *sc*RNF122, Co-IP assays were performed. A prominent band corresponding to *sc*RNF122 was detected in the Flag-*sc*STING immunoprecipitated protein complex (Figure 2G). Similarly, a clear band for *sc*STING was observed in the Myc-*sc*RNF122 immunoprecipitated complex (Figure 2H), confirming their interaction. Segmental analysis of *sc*STING further revealed that the interaction was mediated through the 141–417 amino acid region (Figure 2I). These results indicate that *sc*RNF122 exerts its inhibitory effect on IFN signaling by binding to the 141–417 amino acid region of scSTING.

***sc*RNF122 targets the 94-180 amino acid region of STING for ubiquitination and subsequent degradation**

To elucidate the role of *sc*RNF122 in modulating *sc*STING stability, WB analyses were performed to assess *sc*STING levels and investigate its ubiquitination and degradation. Results showed that co-transfection of *sc*STING and *sc*RNF122 led to a significant reduction in *sc*STING levels in cells expressing *sc*RNF122 (Figure 3A). Moreover, this effect was dose-dependent, with increasing levels of scRNF122 expression leading to progressive depletion of *sc*STING (Figure 3B). To investigate the mechanism underlying *sc*RNF122-induced *sc*STING degradation, the co-transfected cells were treated with various inhibitors, including the proteasome inhibitor MG132, autophagy inhibitor 3-MA, and lysosomal inhibitors CQ and NH_4Cl. Among these, MG132 effectively prevented *sc*RNF122-mediated *sc*STING degradation (Figure 3C). Dose-response experiments confirmed the dose-dependent inhibitory effects of MG132 on *sc*STING degradation (Figure 3D). These observations suggested that *sc*RNF122 promoted *sc*STING degradation through ubiquitination. Consistent with this hypothesis, ubiquitination assays revealed significantly higher levels of

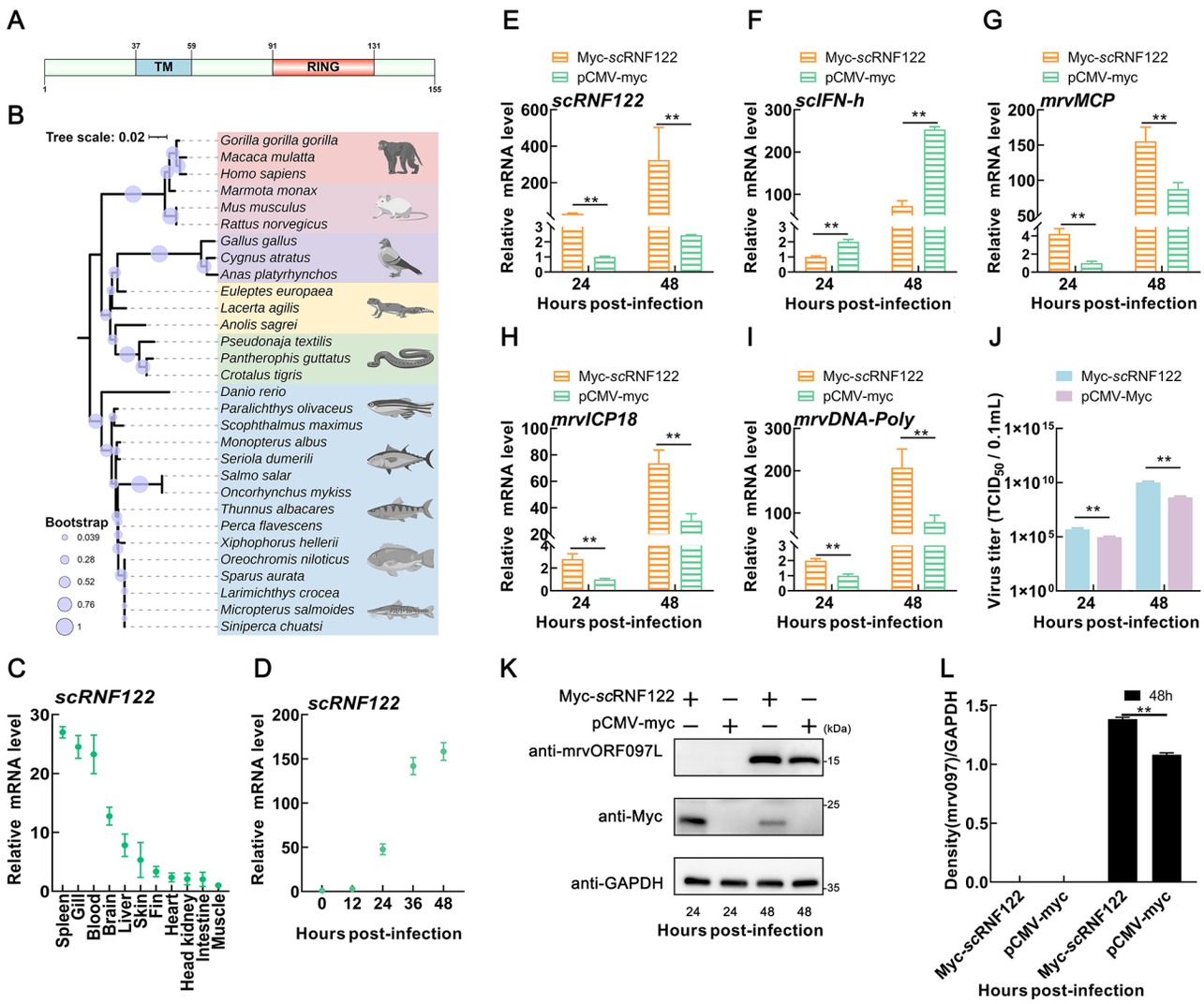

Figure 1 Characterization of *sc*RNF122 and its role in promoting viral replication

A: Predicted domain structure of *sc*RNF122. B: Phylogenetic analysis of RNF122 sequences from representative vertebrate species (GenBank accession numbers are provided in Supplementary Table S3). C: Tissue distribution of *sc*RNF122 protein expression in healthy mandarin fish. Total RNA was extracted from blood, brain, liver, spleen, fin, gill, intestine, heart, skin, head kidney, and muscle samples obtained from three healthy mandarin fish, with *sc*RNF122 expression quantified by RT-qPCR. D: Induction of *sc*RNF122 in MFF-1 cells following MRV infection (multiplicity of infection (MOI) of 0.1), with *sc*RNF122 mRNA expression determined by RT-qPCR and normalized to *β-actin*. Cells were transfected with Myc-*sc*RNF122 or pCMV-Myc for 24 h, then infected with MRV and harvested at indicated time points. E–I: RT-qPCR quantification of *sc*RNF122, *scIFN-h*, *mrvMCP*, *mrvICP18*, and *mrvDNA-Poly* expression in MRV-infected cells at indicated times. Expression values were normalized to the lowest-expressing group, set to 1. J: Viral titers determined by endpoint dilution assay in 96-well culture plates. K: Detection of mrvORF097L protein levels by WB analysis. L: Densitometric quantification of mrvORF097L normalized to GAPDH. Vertical bars represent ±SD (n=3). **: P<0.01.

*sc*STING ubiquitination in the presence of *sc*RNF122 compared to controls (Figure 3E). Taken together, these results indicate that *sc*RNF122 targets *sc*STING for degradation via the ubiquitin-proteasome pathway.

To pinpoint this specific ubiquitination site, a series of truncated *sc*STING variants were generated (Figure 3F) and subjected to degradation assays. Results showed that *sc*RNF122 selectively targeted the N-terminal segment of *sc*STING (1–180 amino acids) for degradation, with the C-terminal region (181–417 amino acids) remaining stable (Figure 3G, H). Further refinement using N-terminal truncations revealed that constructs spanning residues 1–140, 1–134, 1–121, and 1–116 were all susceptible to degradation, while the variant containing residues 1–94 was unaffected (Figure 3J–N), implying that the ubiquitination sites reside within the 94–180 amino acid region of *sc*STING. Supporting this conclusion, scRNF122 induced strong ubiquitination of the scSTING(1–180) fragment but not of the scSTING(181–417) fragment (Figure 3I), confirming that the ubiquitination sites are confined within the 94–180 amino acid segment.

*sc*RNF122 mediates *sc*STING ubiquitination at three specific lysine residues

Ubiquitination primarily targets lysine residues, although cysteine residues may also be modified (Hershko & Ciechanover, 1998). To determine whether *sc*RNF122 specifically targets lysine residues for scSTING ubiquitination, a mutant construct, *sc*STINGCKR, was generated by replacing all cysteine (C) and lysine (K) residues with arginine (R) (Figure 4A). An additional mutant, *sc*STING(1–180)KR, with all K residues in the N-terminal 1–180 amino acids substituted with R, was also constructed. Degradation assays

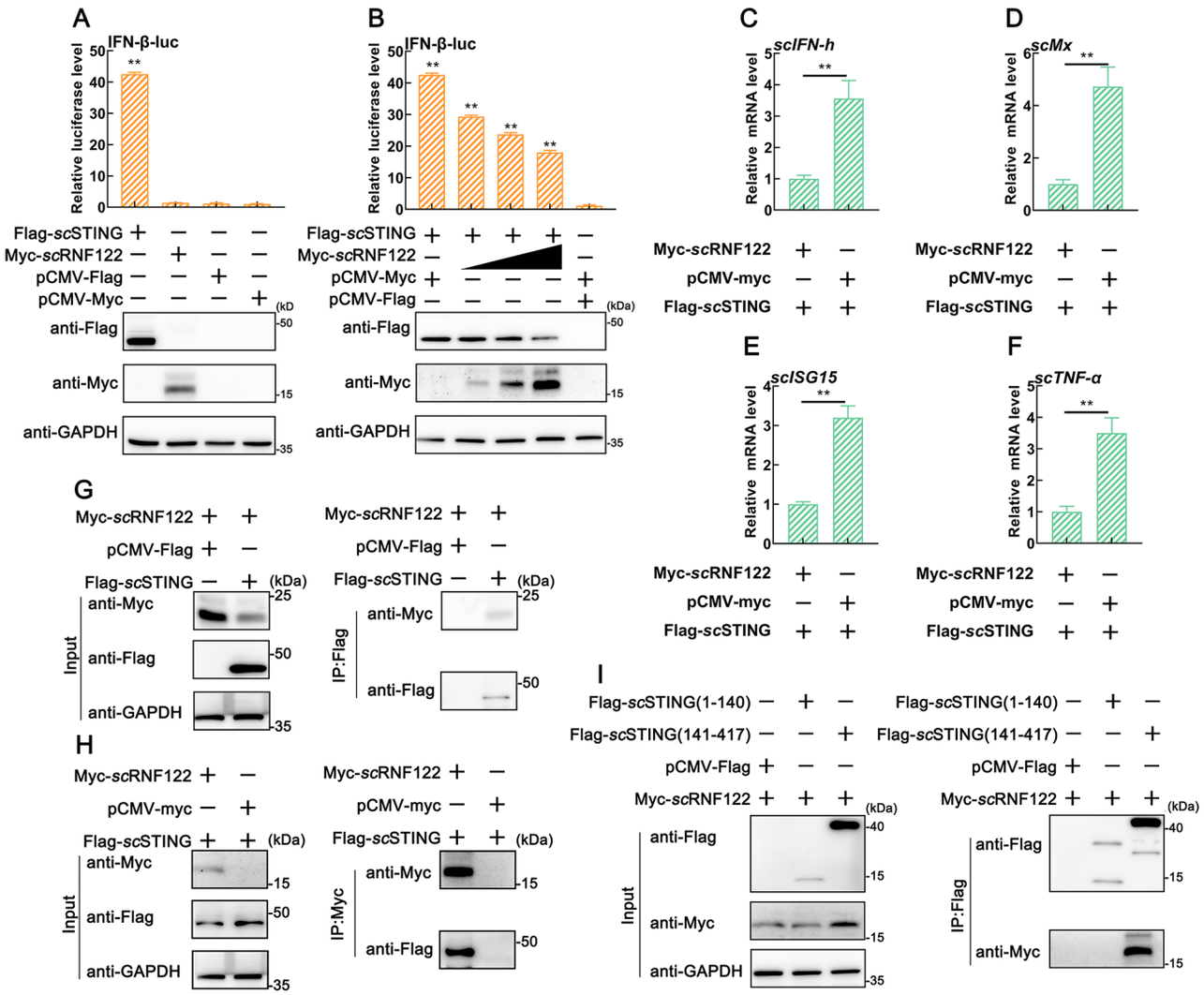

Figure 2 *sc*RNF122 inhibits *sc*STING-induced IFN signaling and physically interacts with *sc*STING

A: Relative IFN-β-luc activity was measured in cells co-transfected with Flag-*sc*STING and Myc-*sc*RNF122. Cells transfected with pCMV-Myc alone served as the negative control. B: MFF-1 cells were co-transfected with pRL-TK and IFN-β-luc reporter plasmids, along with *sc*RNF122 and *sc*STING expression plasmids in 24-well plates. Luciferase activity was assessed 36 h post-transfection. Vertical bars represent ±SD (n=3). **: P<0.01. C–F: mRNA expression levels of *scIFN-h* (C), *scMx* (D), *scISG15* (E), and *scTNF-α* (F) were quantified by RT-qPCR 24 h after co-transfection with scSTING and scRNF122 or vector. Data represent three independent experiments (n=3). **: P<0.01. G, H: FHM cells were transfected with corresponding plasmids or empty vectors, followed by Co-IP and WB analyses to examine the interaction between *sc*RNF122 and *sc*STING. IB: Immunoblotting; IP: Immunoprecipitation. I: FHM cells were co-transfected with pCMV-Myc-*sc*RNF122 or empty vector, pCMV-Flag-*sc*STING(1–140), and pCMV-Flag-*sc*STING(141–417) plasmids. Co-IP and WB analyses were performed to map interaction regions.

demonstrated that *sc*RNF122 failed to degrade either *sc*STINGCKR (Figure 4B) or *sc*STING(1–180)KR (Figure 4C), suggesting that *sc*RNF122-mediated ubiquitination of *sc*STING is lysine-specific. The 1–180 amino acid region of *sc*STING contains six K residues. To identify which are targeted, a series of truncated rescue constructs was generated based on *sc*STINGCKR(1–180), each restoring a single original lysine, including *sc*STINGCKR(1–101)95K, *sc*STINGCKR(1–123)117K, *sc*STINGCKR(1–128)122K, *sc*STINGCKR(1–141)135K, and *sc*STINGCKR(1–161)155K. Co-transfection experiments revealed that *sc*RNF122 selectively degraded the 95K, 117K, and 155K rescue mutants (Figure 4D, G, H), whereas constructs restoring 122K and 135K were resistant to degradation (Figure 4E, F), identifying K95, K117, and K155 as the primary ubiquitination targets. To validate these findings in full-length *sc*STING, six mutants were generated from STINGCKR, including *sc*STINGCKR20K, *sc*STINGCKR95K, *sc*STINGCKR117K, *sc*STINGCKR122K, *sc*STINGCKR135K, and *sc*STINGCKR155K (Figure 4I). Co-transfection experiments showed that *sc*RNF122 failed to degrade *sc*STINGCKR20K, *sc*STINGCKR122K, and *sc*STINGCKR135K (Figure 4J, M, N), but successfully induced degradation of K95, K117, and K155 (Figure 4K, L, O). In addition, *sc*RNF122 also degraded human STING in a dose-dependent manner in L02 cells (Figure 4P). These results indicate that *sc*RNF122 catalyzes the ubiquitination of *sc*STING specifically at lysine residues K95, K117, and K155.

To further dissect the relative contributions of these lysine residues, individual lysine-to-arginine mutations were introduced to generate *sc*STINGK95R, *sc*STINGK117R, and *sc*STINGK155R, along with a triple mutant *sc*STINGK95/117/155R (Figure 5A). Co-transfection of these mutants with *sc*RNF122 revealed that the single mutants remained susceptible to degradation, whereas the triple

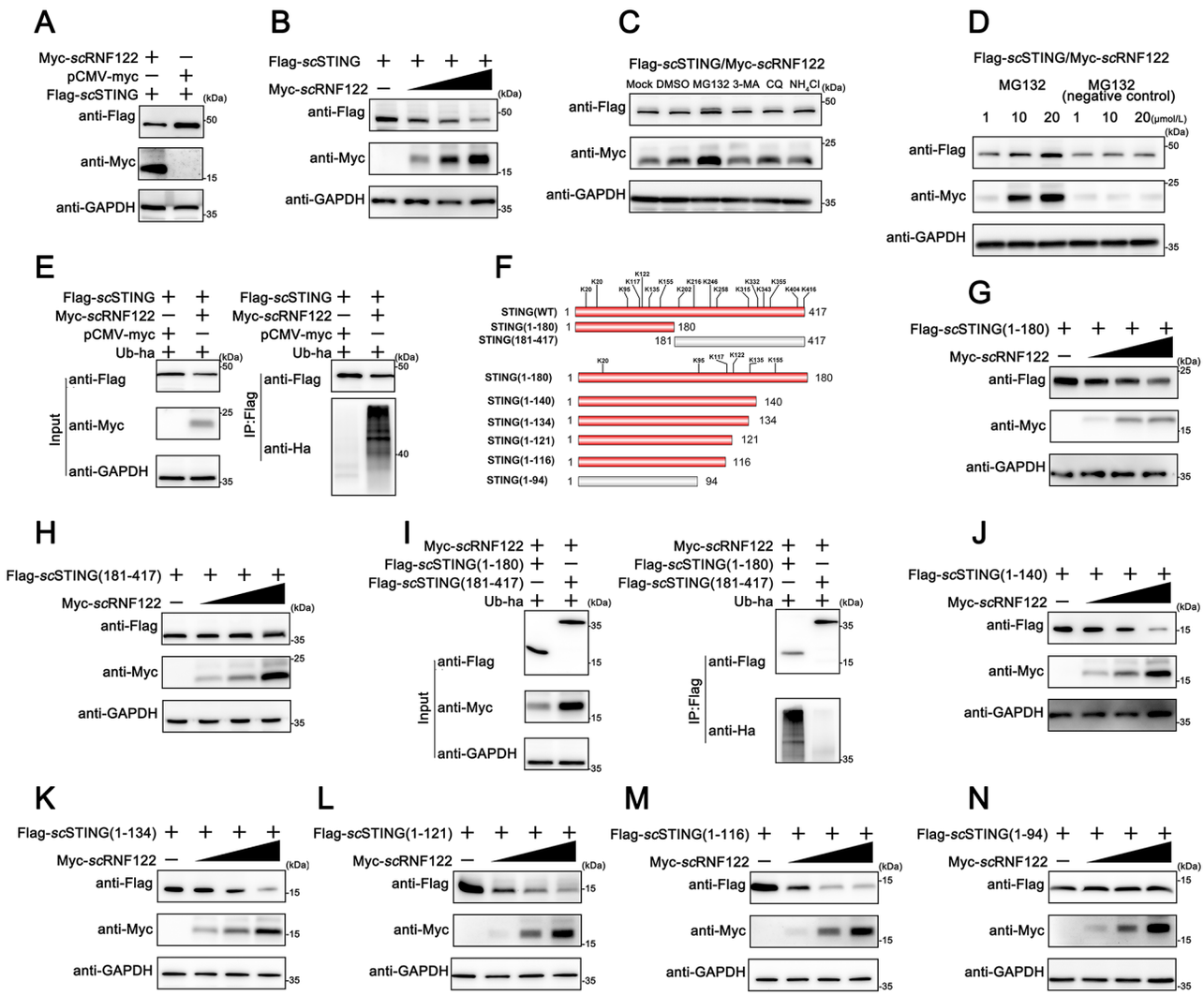

Figure 3 *sc*RNF122 mediates *sc*STING degradation via ubiquitination targeting the 94–180 amino acid region

A: WB analyses were used for detection. FHM cells were transfected with pCMV-Myc-*sc*RNF122 or an empty vector alongside pCMV-Flag-*sc*STING plasmids. B: FHM cells were seeded in 6-well plates, incubated overnight, and co-transfected with 2 μg Flag-*sc*STING and Myc-*sc*RNF122 (0.5, 1, and 2 μg), After 24 h, lysates were immunoblotted with anti-Flag, anti-Myc, and anti-GAPDH antibodies. C: Effects of MG132, 3-MA, CQ, and NH_4Cl on *sc*RNF122-induced *sc*STING degradation were assessed by treating FHM cells in 6-well plates with 2 μg of Flag-*sc*STING and 2 μg of Myc-*sc*RNF122. At 24 h post-transfection (hpt), cells were treated with DMSO or respective inhibitors (MG132: 20 μmol/L, 3-MA: 5 μmol/L, CQ: 10 μmol/L, NH_4Cl: 20 μmol/L). After 12 h, lysates were immunoblotted using anti-Flag, anti-Myc, and anti-GAPDH antibodies. D: FHM cells were transfected and treated with increasing MG132 concentrations (1, 10, and 20 μmol/L), and a negative control (MG132). Lysates were immunoblotted as before. E: Ubiquitination of *sc*STING was assessed in FHM cells co-expressing Flag-*sc*STING, Ha-ubiquitin, and either Myc-*sc*RNF122 (lane 2) or empty vector (lane 1). Flag-*sc*STING was immunoprecipitated with anti-Flag, and poly-ubiquitin chains were detected with anti-Ha. F: Positions of lysine (K) residues in truncated STING variants. G, H: FHM cells were seeded overnight in 6-well plates and co-transfected with 2 μg of either Flag-*sc*STING(1–180) or Flag-*sc*STING(181–417), along with Myc-*sc*RNF122 at concentrations of 0.5, 1, or 2 μg. After 24 h, lysates were immunoblotted using anti-Flag, anti-Myc, and anti-GAPDH antibodies. I: Ubiquitination of *sc*STING fragments was assessed by co-transfecting FHM cells with Myc-*sc*RNF122, Ha-ubiquitin, and either Flag-*sc*STING(1–180) or Flag-*sc*STING(181–417). Flag-scSTING was immunoprecipitated using anti-Flag, and poly-ubiquitin chains were detected with anti-Ha. J–N: Similarly, FHM cells were seeded and co-transfected as in C, but with Flag-*sc*STING(1–140), Flag-*sc*STING(1–134), Flag-*sc*STING(1–121), Flag-*sc*STING(1–116), or Flag-*sc*STING(1–94). Lysates were analyzed by immunoblotting as described above.

mutant was resistant (Figure 5B). Ubiquitination assays confirmed that *sc*STING ubiquitination mediated by *sc*RNF122 significantly decreased with increasing STING site mutations (Figure 5C). Luciferase assays further showed that IFN activation was partially restored by single-site mutations, with the K155 mutant exhibiting the strongest restoration (Figure 5D). These findings indicate that *sc*RNF122 is capable of ubiquitinating all three lysine residues —K95, K117, and K155. However, mutation at K155 results in a markedly greater restoration of IFN activity than mutations at K95 or K117, suggesting that K155 serves as the dominant site mediating *sc*RNF122-dependent suppression of STING signaling.

To explore the differences in *sc*RNF122-mediated K residue targeting *sc*STING between mammals and other vertebrates, homologous sequences of STING were compared across mammals, birds, reptiles, amphibians, and fish. Notably, lysine 155 (K155) in fish STING exhibited high homology with the

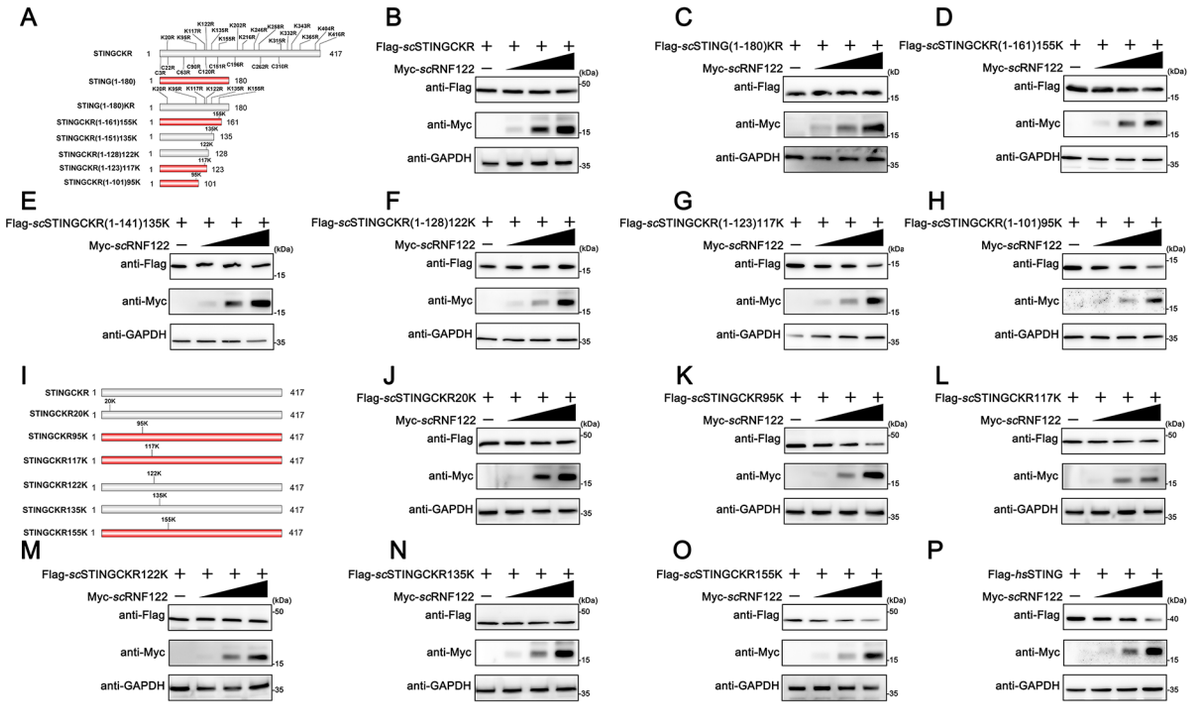

Figure 4 *sc*RNF122 targets *sc*STING for ubiquitination at K95, K117, and K155

A: Schematic of *sc*STING mutants used in this study. B, C: FHM cells were co-transfected with 2 μg of Flag-*sc*STINGCKR/Flag-*sc*STING(1–180)KR and Myc-*sc*RNF122 (0.5, 1 and 2 μg) for 24 h. Lysates were then subjected to immunoblotting with anti-Flag, anti-Myc, and anti-GAPDH Abs. D–H: FHM cells were co-transfected with 2 μg of various Flag-tagged *sc*STING mutants, including *sc*STINGCKR(1–161)155K, *sc*STINGCKR(1–141)135K, *sc*STINGCKR(1–128)122K, *sc*STINGCKR(1–123)117K, and *sc*STINGCKR(1–101)95K, along with Myc-*sc*RNF122 (0.5, 1, and 2 μg) for 24 h. Lysates were then immunoblotted with anti-Flag, anti-Myc, and anti-GAPDH Abs. I: Additional schematic of *sc*STING mutants employed in this study. J–O: FHM cells were seeded and co-transfected as in B, but with specific *sc*STINGCKR mutants: *sc*STINGCKR20K, *sc*STINGCKR95K, *sc*STINGCKR117K, *sc*STINGCKR122K, *sc*STINGCKR135K and *sc*STINGCKR155K. Lysates were processed for immunoblotting. P: L02 cells were seeded and co-transfected as in B, but with *hs*STING. Lysates were analyzed as described above.

highly conserved K150 in other vertebrates (Figure 5E), suggesting functional conservation of this site in negative regulation. In contrast, lysine residues at 95 and 117 were predominantly conserved within Perciformes, indicating that distinct regulatory features may exist among teleost lineages relative to other vertebrates.

*sc*RNF122 negatively regulates *sc*STING-mediated antiviral activity

To assess the impact of *sc*RNF122 on *sc*STING-mediated antiviral defense, MFF-1 cells co-expressing both proteins were subjected to MRV infection. Viral loads in the collected supernatants were quantified, and cellular samples were analyzed by RT-qPCR and WB. Co-expression of *sc*STING and *sc*RNF122 (Figure 6A, B) resulted in increased transcription of the *scIFN-h* gene (Figure 6C), alongside elevated expression of MRV genes *mrvMCP*, *mrvICP18*, and *mrvDNA-Poly* (Figure 6D–F). In addition, viral titers ($TCID_{50}$) and levels of viral protein mrvORF097L were significantly higher in the co-expression group compared to cells expressing *sc*STING alone (Figure 6G, H). Collectively, these results demonstrate that *sc*RNF122 attenuates *sc*STING-dependent antiviral signaling.

DISCUSSION

This study demonstrated that RNF122 exerted an inhibitory effect on the STING-mediated IFN signaling pathway in mandarin fish, impairing STING-driven antiviral responses by facilitating its degradation through the ubiquitin-proteasome pathway at lysine residues K95, K117, and K155 (Figure 7). These findings elucidate a previously uncharacterized regulatory mechanism of STING activity in teleosts and provide a molecular basis for modulating antiviral immunity in aquatic species, offering potential strategies for the development of disease-resistant strains and immunomodulatory therapeutics.

Although IFNs are essential components of the innate immune system, their excessive production can provoke pathological inflammation, leading to severe outcomes. Therefore, tight regulation of IFN signaling is vital for preserving immune homeostasis (Jefferies, 2019). TRIM56 promotes K63-linked ubiquitination at the K150 residue of STING, facilitating the activation of the STING/IFN signaling pathway (Tsuchida et al., 2010), while RNF5 inhibits K48-linked ubiquitination at the K150 residue, directing STING toward proteasomal degradation (Zhong et al., 2009). In this study, RNF122 was shown to negatively regulate STING activity in mandarin fish by enhancing its ubiquitination and degradation.

The contribution of RNF family members to antiviral immunity has gained increasing recognition. For instance, RNF144A is up-regulated following HSV-1 infection, which amplifies innate immune reactions triggered by DNA viruses (Yang et al., 2023). Conversely, LjRNF114, induced by

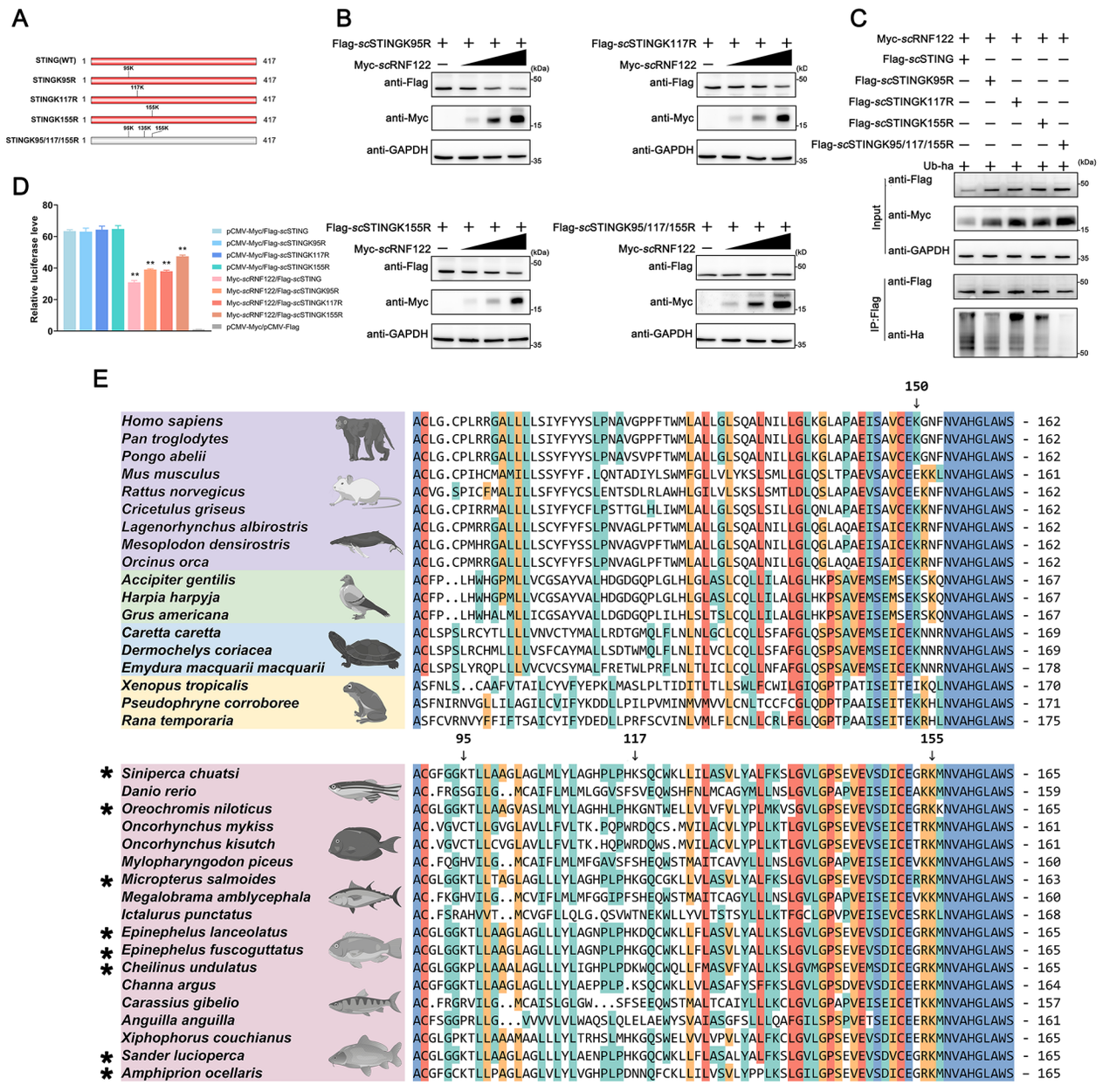

Figure 5 *sc*RNF122 ubiquitinates specific lysine residues (K95, K117, and K155) of *sc*STING

A: Schematic representation of *sc*STING mutants used in this study. B: FHM cells were co-transfected with 2 μg of Flag-*sc*STING mutants (K95R, K117R, K155R, and K95/117/155R) and increasing amounts of Myc-tagged *sc*RNF122 (0.5, 1, and 2 μg) for 24 h. Cell lysates were then subjected to immunoblotting with anti-Flag, anti-Myc, and anti-GAPDH antibodies. C: Ubiquitination of *sc*STING mutants (K95R, K117R, K155R, and K95/117/155R) was assessed. FHM cells were co-expressed with Myc-*sc*RNF122, Ha-ubiquitin, and either Flag-*sc*STING, Flag-*sc*STINGK95R, Flag-*sc*STINGK117R, Flag-*sc*STINGK155R, or Flag-*sc*STINGK95/117/155R. Flag-*sc*STING was immunoprecipitated using anti-Flag, and poly-ubiquitin chains were detected with anti-Ha. D: MFF-1 cells were co-transfected in 24-well plates with reporter plasmids pRL-TK and IFN-β-luc, along with plasmids encoding *sc*RNF122 or pCMV-Myc and *sc*STING mutants. Luciferase activity was measured 36 h post-transfection. E: Protein amino acid alignment revealed conserved amino acid sequences and distribution of lysine sites in STING across different species. Accession numbers for these sequences are provided in Supplementary Table S3. Arrows indicate lysine residues at positions 95, 117, and 155 in *sc*STING. Asterisk (*) represents fish belonging to the order Perciformes.

infection with red-spotted grouper nervous necrosis virus, attenuates antiviral signaling through the RLR pathways, facilitating immune evasion and viral infection (Xiang et al., 2021). In this context, the present findings demonstrated that MRV infection up-regulated RNF122 expression in mandarin fish cells. Notably, RNF122 expression was also enriched in immune-relevant tissues, including spleen and blood, supporting its pivotal role in modulating the innate immune response during viral challenge.

E3 ubiquitin ligases serve as critical modulators of the antiviral innate immune response by orchestrating the post-translational regulation of IFN-I production (Schneider et al., 2014). Among these, RNF114 suppresses IFN-I induction by interacting with MAVS and impairing antiviral responses

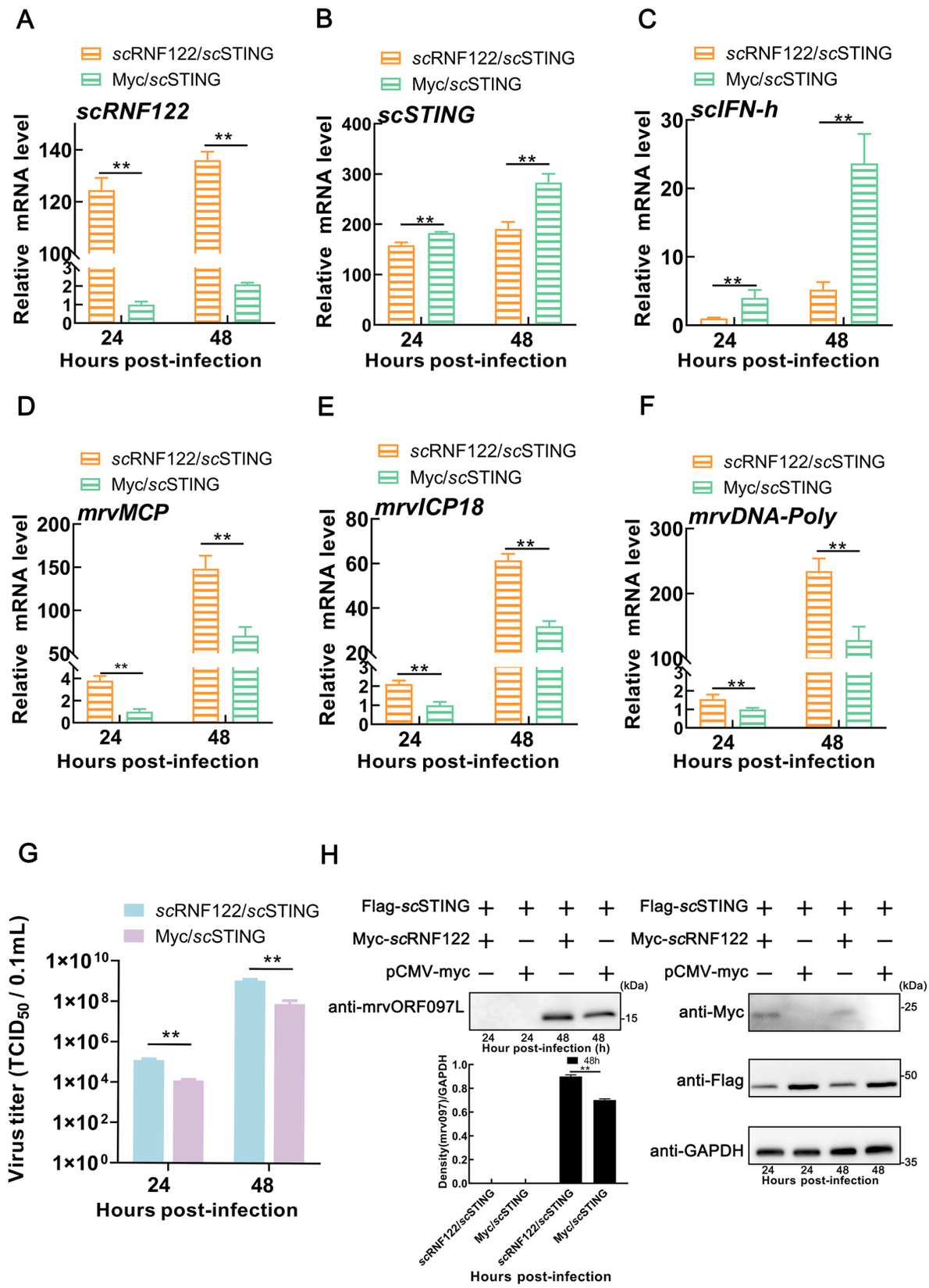

Figure 6 *sc*RNF122 inhibits *sc*STING-mediated antiviral activity

A–F: MFF-1 cells were infected with MRV and harvested at the indicated time points for RT-qPCR, WB, and $TCID_{50}$ analyses. Expression levels of *sc*RNF122 (A), *sc*STING (B), *scIFN-h* (C), *mrvMCP* (D), *mrvICP18* (E), and *mrvDNA-Poly* (F) in MRV-infected cells at indicated times. For RT-qPCR, the baseline was set as the group with the lowest relative expression among all groups, assigned a value of 1. Each group represented different time points after viral infection. G: Virus titers were determined using the endpoint dilution method. H: WB analysis was performed to assess levels of the viral protein mrvORF097L, with densitometric quantification normalized to GAPDH. Left two lanes represent samples collected at 24 hpi, while right two lanes indicate samples collected 48 hpi. Vertical bars represent ±SD (n=3). **: P<0.01.

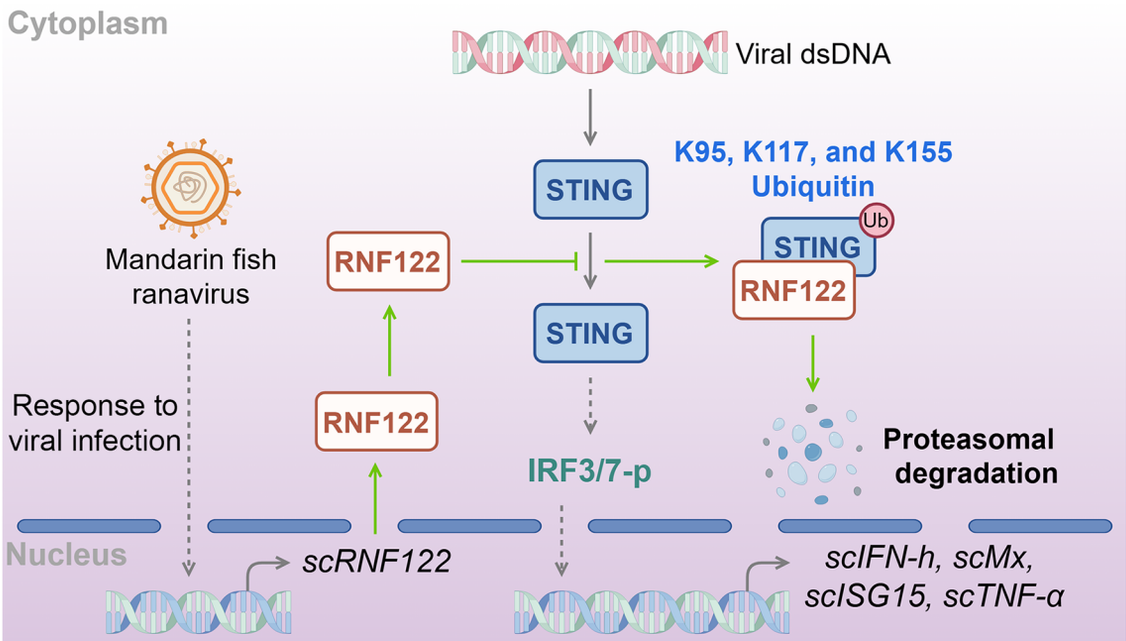

Figure 7 Schematic representation of RNF122-mediated negative regulation of STING signaling in mandarin fish

*sc*RNF122 interacted with *sc*STING and catalyzed ubiquitination at lysine residues K95, K117, and K155. This post-translational modification targeted *sc*STING for proteasomal degradation, thereby preventing IFN signaling. Through targeted degradation of *sc*STING, *sc*RNF122 impaired the host antiviral response and promoted viral replication.

during vesicular stomatitis virus (VSV) infection, thereby facilitating viral replication (Han et al., 2022). In contrast, RNF123 enhances IFN-I expression in duck Tembusu viral infection by facilitating TLR3/IRF7 signaling through the degradation of SOCS1, ultimately restricting viral replication (Huang et al., 2023). RNF122 has also emerged as a negative regulator of the RIG-I pathway, targeting the CARD of RIG-I for ubiquitin-mediated degradation (Wang et al., 2016). In pigs, RNF122 promotes MDA-5 ubiquitination and degradation to support porcine reproductive and respiratory syndrome virus replication (Sun et al., 2022), while in carp, RNF122-like protein facilitates spring viremia of carp virus replication by triggering STING degradation via ubiquitination (Liu et al., 2024). Consistent with these roles, our results demonstrated that RNF122 inhibits STING-induced IFN-I production and promotes MRV replication in mandarin fish.

Despite the central role of E3 ligases in shaping antiviral immunity, the identification of precise ubiquitination sites —particularly in non-mammalian vertebrates —remains limited. Prior studies have shown that the RING finger domain of RNF122 mediates ubiquitin transfer to lysine residues K115 and K146 within the CARD of RIG-I (Wang et al., 2016). In the current work, RNF122 was shown to target STING for ubiquitination at lysine residues K95, K117, and K155 in mandarin fish. Notably, RNF122 also induced the degradation of human STING in a dose-dependent manner, indicating a conserved regulatory function across vertebrates. Sequence comparison revealed that K155 in teleost STING shared homology with mammalian K150, while K95 and K117 were only found in Perciformes. This lineage-specific pattern of lysine conservation suggests that RNF122 may modulate STING activity through distinct mechanisms in different fish clades. Such targeted regulation of inflammatory signaling could contribute to enhanced immune tolerance and potentially support increased healthspan in certain teleost lineages (Wang et al., 2024).

While our study offers significant insights into the role of RNF122 in regulating STING-mediated immune responses, several limitations need to be recognized. Firstly, our findings were primarily based on *in vitro* experiments, and their physiological relevance *in vivo* remains to be established. Future studies should prioritize *in vivo* validation using appropriate animal models to assess the functional consequences of RNF122 modulation in more complex biological systems. Targeted gene knockout experiments, such as RNF122 knockout via CRISPR/Cas9, should also be conducted to further clarify the impact of RNF122 deficiency on STING signaling and antiviral immunity. Additionally, investigating the potential of RNF122 as a therapeutic target in aquaculture presents a promising avenue. Strategies such as the development of RNF122-specific inhibitors or the generation of RNF122-deficient fish lines may offer valuable approaches to enhance viral resistance in commercially important teleost species. Given the apparent contribution of RNF122 to dampening inflammatory signaling, such interventions may also support improved immune resilience and healthspan in farmed fish (Wang et al., 2024). These future directions will be essential for evaluating the translational potential of RNF122-targeted manipulation for controlling viral infections in aquaculture settings.

SUPPLEMENTARY DATA

Supplementary data to this article can be found online.

COMPETING INTERESTS

The authors declare that they have no competing interests.

AUTHORS' CONTRIBUTIONS

X.W.Q.: Formal analysis, Investigation, Data curation, Visualization, Writing–original draft. C.R.L.: Formal analysis, Data curation, Investigation. M.C.L.: Formal analysis, Visualization. T.H.L.: Investigation, Data curation. Y.L.Y.: Investigation, Resources. S.P.W.: Investigation, Resources. J.G.H.: Resources, Funding acquisition, Project administration. C.J.G.: Conceptualization, Formal analysis, Funding acquisition, Project administration, Visualization, Writing–review and editing. All authors read and approved the final version of the manuscript.

ACKNOWLEDGEMENTS

We gratefully acknowledge all study participants and individuals who contributed to this study. We also thank www.figdraw.com for illustrative components.

REFERENCES

Benson DA, Cavanaugh M, Clark K, et al. 2013. GenBank. *Nucleic Acids Research*, **41**(D1): D36–D42.

Bhoj VG, Chen ZJ. 2009. Ubiquitylation in innate and adaptive immunity. *Nature*, **458**(7237): 430–437.

Dong CF, Wang ZM, Weng SP, et al. 2017. Occurrence of a lethal ranavirus in hybrid mandarin (*Siniperca scherzeri*× *Siniperca chuatsi*) in Guangdong, South China. *Veterinary Microbiology*, **203**: 28–33.

Dong CF, Weng SP, Shi XJ, et al. 2008. Development of a mandarin fish *Siniperca chuatsi* fry cell line suitable for the study of infectious spleen and kidney necrosis virus (ISKNV). *Virus Research*, **135**(2): 273–281.

Han WZ, Chen Q, Cui J, et al. 2022. E3 ubiquitin ligase RNF114 promotes vesicular stomatitis virus replication via inhibiting type I interferon production. *Microbial Pathogenesis*, **167**: 105569.

Hershko A, Ciechanover A. 1998. The ubiquitin system. *Annual Review of Biochemistry*, **67**: 425–479.

Hopfner KP, Hornung V. 2020. Molecular mechanisms and cellular functions of cGAS–STING signalling. *Nature Reviews Molecular Cell Biology*, **21**(9): 501–521.

Huang SZ, Cui M, Huang J, et al. 2023. Rnf123 mediates ubiquitination and degradation of socs1 to regulate type I interferon production during duck tembusu virus infection. *Journal of Virology*, **97**(4): e0009523.

Ishikawa H, Barber GN. 2008. STING is an endoplasmic reticulum adaptor that facilitates innate immune signalling. *Nature*, **455**(7213): 674–678.

Ishikawa H, Ma Z, Barber GN. 2009. STING regulates intracellular DNA-mediated, type I interferon-dependent innate immunity. *Nature*, **461**(7265): 788–792.

Jefferies CA. 2019. Regulating IRFs in IFN driven disease. *Frontiers in Immunology*, **10**: 325.

Jiang S, Li HQ, Zhang LWY, et al. 2025. Generic Diagramming Platform (GDP): a comprehensive database of high-quality biomedical graphics. *Nucleic Acids Research*, **53**(D1): gkae973.

Letunic I, Bork P. 2024. Interactive Tree of Life (iTOL) v6: recent updates to the phylogenetic tree display and annotation tool. *Nucleic Acids Research*, **52**(W1): gkae268.

Letunic I, Khedkar S, Bork P. 2021. SMART: recent updates, new developments and status in 2020. *Nucleic Acids Research*, **49**(D1): D458–D460.

Li ZM, Qin XW, Zhang Q, et al. 2024. Mandarin fish von Hippel-Lindau protein regulates the NF-κB signaling pathway via interaction with IκB to promote fish ranavirus replication. *Zoological Research*, **45**(5): 990–1000.

Liu RR, Meng F, Liu TT, et al. 2024. RING finger protein 122-like (RNF122L) negatively regulates antiviral immune response by targeting STING in common carp (*Cyprinus carpio* L.). *International Journal of Biological Macromolecules*, **269**: 132104.

O'Leary NA, Wright MW, Brister JR, et al. 2016. Reference sequence (RefSeq) database at NCBI: current status, taxonomic expansion, and functional annotation. *Nucleic Acids Research*, **44**(D1): D733–D745.

Pan J, Fei CJ, Hu Y, et al. 2023. Current understanding of the cGAS-STING signaling pathway: Structure, regulatory mechanisms, and related diseases. *Zoological Research*, **44**(1): 183–218.

Pan WQ, Liang MC, You YL, et al. 2024. Viral genomic methylation and the interspecies evolutionary relationships of ranavirus. *PLoS Pathogens*, **20**(11): e1012736.

Phelan T, Little MA, Brady G. 2020. Targeting of the cGAS-STING system by DNA viruses. *Biochemical Pharmacology*, **174**: 113831.

Qin XW, He J, Yu Y, et al. 2020. The roles of mandarin fish STING in innate immune defense against infectious spleen and kidney necrosis virus infections. *Fish & Shellfish Immunology*, **100**: 80–89.

Reed LJ, Muench H. 1938. A simple method of estimating fifty per cent endpoints. *American Journal of Epidemiology*, **27**(3): 493–497.

Schneider WM, Chevillotte MD, Rice CM. 2014. Interferon-stimulated genes: a complex web of host defenses. *Annual Review of Immunology*, **32**: 513–545.

Sun RQ, Guo YY, Li XY, et al. 2022. PRRSV non-structural proteins orchestrate porcine E3 ubiquitin ligase RNF122 to promote PRRSV proliferation. *Viruses*, **14**(2): 424.

Tamura K, Stecher G, Kumar S. 2021. MEGA11: molecular evolutionary genetics analysis version 11. *Molecular Biology and Evolution*, **38**(7): 3022–3027.

Tsuchida T, Zou J, Saitoh T, et al. 2010. The ubiquitin ligase TRIM56 regulates innate immune responses to intracellular double-stranded DNA. *Immunity*, **33**(5): 765–776.

Wang WD, Jiang MH, Liu S, et al. 2016. RNF122 suppresses antiviral type I interferon production by targeting RIG-I CARDs to mediate RIG-I degradation. *Proceedings of the National Academy of Sciences of the United States of America*, **113**(34): 9581–9586.

Wang X, Jia JK, Wang Q, et al. 2024. *Myotis* bat STING attenuates aging-related inflammation in female mice. *Zoological Research*, **45**(5): 961–971.

Xiang YX, Zhang WW, Jia P, et al. 2021. E3 ubiquitin ligase RNF114 inhibits innate immune response to red-spotted grouper nervous necrosis virus infection in sea perch by targeting MAVS and TRAF3 to mediate their degradation. *The Journal of Immunology*, **206**(1): 77–88.

Yang B, Pei JY, Lu C, et al. 2023. RNF144A promotes antiviral responses by modulating STING ubiquitination. *EMBO Reports*, **24**(12): e57528.

Yu Y, He J, Liu WH, et al. 2023. Molecular characterization and functional analysis of hypoxia-responsive factor prolyl hydroxylase domain 2 in mandarin fish (*Siniperca chuatsi*). *Animals*, **13**(9): 1556.

Zeng RY, Pan WQ, Lin YF, et al. 2021. Development of a gene-deleted live attenuated candidate vaccine against fish virus (ISKNV) with low pathogenicity and high protection. *iScience*, **24**(7): 102750.

Zhong B, Yang Y, Li S, et al. 2008. The adaptor protein MITA links virus-sensing receptors to IRF3 transcription factor activation. *Immunity*, **29**(4): 538–550.

Zhong B, Zhang L, Lei CQ, et al. 2009. The ubiquitin ligase RNF5 regulates antiviral responses by mediating degradation of the adaptor protein MITA. *Immunity*, **30**(3): 397–407.